

# STRAIGHT SKELETONS OF SIMPLE POLYGONS

OSWIN AICHHOLZER

FRANZ AURENHAMMER

Institute for Theoretical Computer Science

Graz University of Technology

Klosterwiesgasse 32/2, A-8010 Graz, Austria

{oaich,auren}@igi.tu-graz.ac.at

DAVID ALBERTS

BERND GÄRTNER

Institut für Informatik

Freie Universität Berlin

Takustraße 9, D-14195 Berlin, Germany

{alberts,gaertner}@inf.fu-berlin.de

**Keywords:** Simple polygon, skeleton, roof construction

**Abstract** A new internal structure for simple polygons, the straight skeleton, is introduced and discussed. It is a tree and partitions the interior of a given  $n$ -gon  $P$  into  $n$  monotone polygons, one for each edge of  $P$ . Its straight-line structure and its lower combinatorial complexity may make the straight skeleton  $S(P)$  preferable to the widely used medial axis of  $P$ . We show that  $S(P)$  has no Voronoi diagram structure and give an  $O(nr \log n)$  time and  $O(n)$  space construction algorithm, where  $r$  counts the reflex vertices of  $P$ . As a seemingly unrelated application, the straight skeleton provides a canonical way of constructing a roof of given slope above a polygonal layout of ground walls.

## 1 Introduction and basic properties

The purpose of this paper is to introduce and discuss a new and interesting internal structure for simple polygons in the plane. The new structure, called the *straight skeleton*, is solely made up of straight line segments which are pieces of angular bisectors of polygon edges. It uniquely partitions the interior of a given  $n$ -gon  $P$  into  $n$  monotone polygons, one for each edge of  $P$ .

The straight skeleton, in general, differs from the well-known *medial axis* of  $P$  which consists of all interior points whose closest point on  $P$ 's boundary is not unique; see e.g. [L]. If  $P$  is convex then both structures are identical. Otherwise, the medial axis contains parabolically curved segments in the neighborhood of reflex vertices of  $P$  which are avoided by the straight skeleton. If  $P$  is rectilinear then the straight skeleton is the medial axis of  $P$  for the  $L_\infty$ -metric.

While the medial axis is a Voronoi-diagram-like concept, the straight skeleton is not defined using a distance function but rather by an appropriate *shrinking process* for  $P$ . Imagine that the boundary of  $P$  is contracted towards  $P$ 's interior, in a self-parallel manner and at the same speed for all edges. Lengths of edges might decrease or increase in this process. Each vertex of  $P$  moves along the angular bisector of its incident edges. This situation continues as long as the boundary does not change topologically. There are two possible types of changes:

- (1) *Edge event*: An edge shrinks to zero, making its neighboring edges adjacent now.

(2) *Split event*: An edge is split, i.e., a reflex vertex runs into this edge, thus splitting the whole polygon. New adjacencies occur between the split edge and each of the two edges incident to the reflex vertex.

After either type of event, we are left with a new, or two new, polygons which are shrunk recursively if they have non-zero area. Note that certain events will occur simultaneously even if  $P$  is in general position, namely three edge events letting a triangle collapse to a point. The shrinking process gives a hierarchy of nested polygons; see Figure 1(a).

The straight skeleton,  $S(P)$ , is defined as the union of the pieces of angular bisectors traced out by polygon vertices during the shrinking process.  $S(P)$  is a unique structure defining a polygonal partition of  $P$ . Each edge  $e$  of  $P$  sweeps out a certain area which we call the *face* of  $e$ . Bisector pieces are called *arcs*, and their endpoints which are not vertices of  $P$  are called *nodes*, of  $S(P)$ . See Figure 1(b).

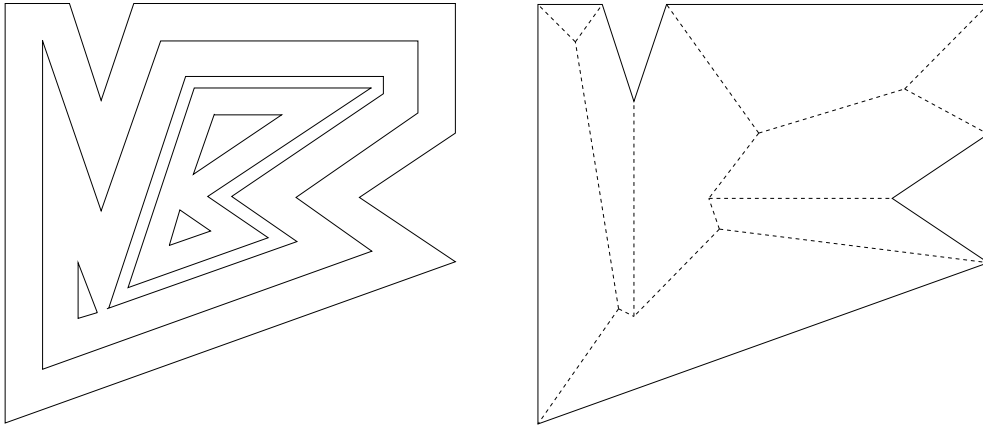


Figure 1: (a) Polygon hierarchy and (b) straight skeleton

As far as it is known to the authors, no attention has been paid to the straight skeleton in the literature. We show that  $S(P)$  has several useful properties. For example, its tree structure implies that, if  $P$  is non-convex,  $S(P)$  is of smaller combinatorial size than the medial axis of  $P$ . The latter, though also being a tree, has to distinguish between curved and straight parts of arcs. As a particularly nice property,  $S(P)$  partitions  $P$  into monotone polygons.

A three-dimensional interpretation of  $S(P)$ , the roof model, is discussed in Section 2 and Section 3. This leads us to the interesting and practically relevant question of constructing a roof of fixed slope above a given layout  $P$  of ground walls. The roof model allow us to gain more insight into the structure of straight skeletons and, in particular, gives a way to define  $S(P)$  non-procedurally. On the other hand,  $S(P)$  provides a canonical way of constructing a roof above  $P$ . We show that the roof corresponding to  $S(P)$  exclusively has the property that rainwater runs off from each roof facet to its defining edge of  $P$ . We also disprove the obvious conjecture that roofs can be expressed as lower envelopes of simply-shaped linear functions. Hence  $S(P)$  is no Voronoi-diagram-like structure, a fact that complicates its algorithmic construction.

An algorithm for computing  $S(P)$  is given in Section 4. It runs in  $O(nr \log n)$  time and  $O(n)$  space if  $P$  is an  $n$ -gon with  $r$  reflex vertices. If no split events occur in the shrinking process for  $P$  then the runtime reduces to  $O(n \log n)$ . Section 5 offers a short discussion of the presented topic.

The rest of this section describes some basic properties of  $S(P)$ .

**Lemma 1**  $S(P)$  is a tree and consists of exactly  $n$  connected faces,  $n - 2$  nodes and  $2n - 3$  arcs.

*Proof.* The construction of a face  $f(e)$  starts at its edge,  $e$ , of  $P$ .  $f(e)$  cannot be split even if  $e$  happens to be. The construction of  $f(e)$  is completed when (every part of)  $e$  has shrunk to zero. As  $e$  cannot reappear again,  $f(e)$  is connected, and  $S(P)$  is acyclic. That is,  $S(P)$  is a tree with the  $n$  vertices of  $P$  as leaves, and has  $n - 2$  nodes and  $2n - 3$  arcs.  $\square$

Two types of arcs of  $S(P)$  can be distinguished. Each arc is a piece of the angular bisector of two edges  $e$  and  $e'$  of  $P$  or, more precisely, of the lines  $\ell(e)$  and  $\ell(e')$  supporting these edges. Note that the angular bisector of  $\ell(e)$  and  $\ell(e')$  actually consists of two lines that intersect at  $\ell(e) \cap \ell(e')$ . We single out the one relevant for  $S(P)$  as follows. Each line  $\ell(e)$  defines a halfplane  $h(e)$  that contains  $P$  near  $e$ . One of the bisector lines intersects the wedge  $h(e) \cap h(e')$  while the other avoids it. We call the former the *bisector* of the edges  $e$  and  $e'$  and will ignore the latter in our considerations. An arc  $a$  defined by this bisector is called a *convex arc* or a *reflex arc* depending on whether its wedge contains  $a$  or not. We also consider  $a$  as labeled by the ordered pair  $(e, e')$ . The order reflects the side of  $a$  where  $\ell(e)$  contributes to the boundary of the wedge.

Each convex (reflex) vertex of  $P$  obviously gives rise to a convex (reflex) arc of  $S(P)$ . While convex arcs can also connect two nodes of  $S(P)$ , this is impossible for reflex arcs.

**Lemma 2** Reflex arcs of  $S(P)$  only emanate from reflex vertices of  $P$ .

*Proof.* Let  $vu$  be an arc emanating from some vertex  $v$  of  $P$ . Then  $u$  is a node which corresponds either to an edge event or to a split event. It suffices to show that, after the event,  $S(P)$  continues at  $u$  with convex arcs only.

In the former case, let  $vw$  be the vanishing edge. Since the arc  $wu$  meets  $vu$  at  $u$ ,  $u$  must be a convex vertex of the shrunk polygon after the event. In the latter case, the polygon splits at  $u$ . It is obvious that, after that event,  $u$  is a convex vertex of both new polygons.

In conclusion, each new vertex generated during the shrinking process is convex. Hence the arcs continuing at  $u$  are contained in their respective wedges which shows their convexity.  $\square$

## 2 Graph model and roof model

It seems hard to give a non-procedural definition of the straight skeleton, as it is available for the medial axis using distances from the boundary. The shrinking model suggests to define the distance of a point  $x \in P$  from an edge  $e$  as the normal distance from  $x$  to the supporting line  $\ell(e)$ . This definition fails as  $e$  might have vanished before  $\ell(e)$  sweeps across  $x$ . Below we discuss two other approaches, the graph model and the roof model, that allow us to gain more insight into the structure of straight skeletons.

$S(P)$  can be seen as a geometric graph whose arcs are pieces of bisectors defined by the edges of  $P$ , each arc being labeled by an ordered pair of edges. Arcs are bounded by  $P$ 's vertices, which have degree 1 in the graph, and by  $S(P)$ 's nodes which have degree 3. Each node is the intersection point of three bisectors. (To ease the discussion, we exclude degeneracies caused

by special shapes of  $P$ .) Its three incident arcs have labels of the form  $(a, b)$ ,  $(b, c)$ ,  $(c, a)$ , and the ordering of each label  $(a, b)$  indicates the position of the faces  $f(a)$  and  $f(b)$  relative to the arc. We call a graph with these properties a *bisector graph* for  $P$ .

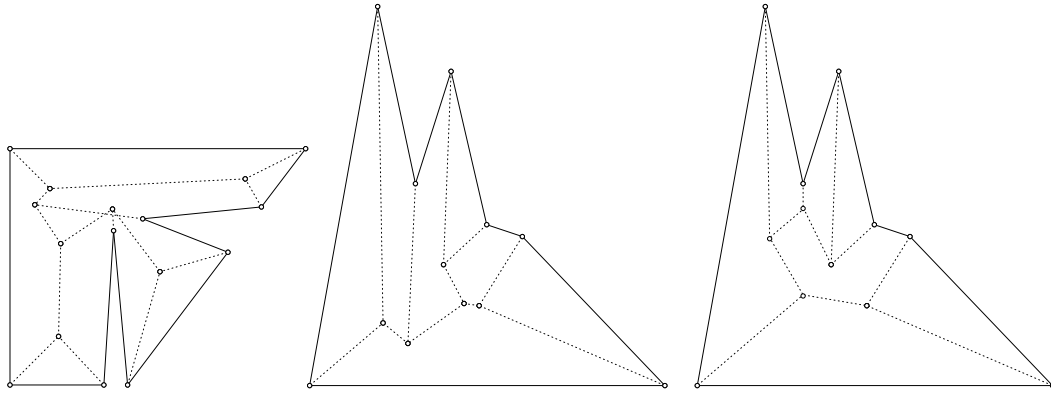


Figure 2: Bisector graphs; self-intersection and ambiguity

However, these properties are far too weak to imply uniqueness. A bisector graph need not even define a partition of  $P$  (and thus a face structure) as long as we do not require it to be plane. Restriction to plane graphs, even to plane trees (as it is the case for  $S(P)$ , see Lemma 1) still gives no unique structure; see Figure 2.

Alternatively, and more intuitively appealing, a plane bisector graph for  $P$  can be viewed as the projection of a three-dimensional object.

Let  $P$  be contained in the horizontal plane  $\Pi_0$ , and associate each edge  $e$  of  $P$  with a halfplane  $\Pi(e)$  in three-space.  $\Pi(e)$  is bounded by  $\ell(e)$ , has a fixed slope (say 45 degrees) with respect to  $\Pi_0$ , and is inclined towards  $P$ . For adjacent edges  $e$  and  $e'$  of  $P$ , the halfline  $\Pi(e) \cap \Pi(e')$  projects vertically to the (relevant halfline of the) bisector of  $e$  and  $e'$ .

We now define a *roof* for  $P$  as a terrain (graph of a piecewise-linear continuous function) over  $P$  whose facets are from the halfplanes above and whose intersection with  $\Pi_0$  is the boundary of  $P$ . Intuitively speaking, this is a 45-degree roof with  $P$ 's edges as ground walls; see Figure 3.

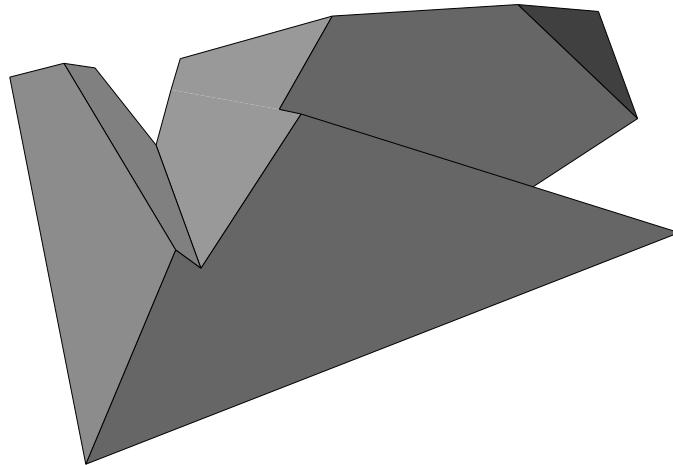


Figure 3: Roof model for straight skeleton in Figure 1

**Theorem 1** *Every roof for  $P$  corresponds to a unique plane bisector graph for  $P$ , and vice versa.*

*Proof.* Let  $R$  be a roof for  $P$ . By the choice of the halfplanes supporting  $R$ 's facets, the edges of  $R$  project vertically to pieces of edge bisectors. Bisectors are labeled correctly, as each node of the resulting graph is the projected intersection of three halfplanes. Finally, the graph is plane as  $R$  is a terrain.

Let  $G$  be a plane bisector graph for  $P$ . Each node  $u$  of  $G$  is the center of a circle that touches three lines supporting the three edges of  $P$  that define  $u$ . We lift up  $u$  vertically by the radius of this circle, getting a point  $\lambda(u)$  in three-space. Note that, if  $u$ 's arcs are labeled  $(a, b)$ ,  $(b, c)$ ,  $(c, a)$ , then  $\lambda(u) \in \Pi(a) \cap \Pi(b) \cap \Pi(c)$ . Let now  $f$  be a face of  $G$ . Each arc bounding  $f$  has a label of the form  $(x, e)$ , where  $x$  runs through the edges defining the faces of  $G$  adjacent to  $f$ . Hence  $\lambda(u) \in \Pi(e)$  for all nodes  $u$  of  $f$ . Clearly,  $e \in \Pi(e)$  by definition. (Note, however, that  $e$  does not necessarily bound  $f$ .) This shows that  $f$  is lifted up by  $\lambda$  to a planar facet. As  $G$  is a plane graph, we obtain a piecewise-linear function over  $P$ . This function is continuous as facets stemming from faces  $f(e)$  and  $f(e')$  touch along the lifted arc with label  $(e, e')$ .  $\square$

In the unique roof of a plane bisector graph, convex arcs of the graph give rise to *ridges* of the roof (both facets going downwards) and reflex arcs give rise to *valleys* (both facets going upwards). Note the impossibility of having one facet upwards and the other downwards. Endpoints of ridges or of valleys that are not polygon vertices are called *corners* of the roof. They lie above plane  $\Pi_0$  and project to the nodes of the graph.

It is interesting – also from a practical point of view – to study which kind of roofs are legitimate by our definition. Surprisingly, a halfplane may contribute more than one facet to the roof. That is, an edge of  $P$  may yield several faces in the bisector graph. Even local minima may arise; see Figure 4. The first anomaly indicates that, in contrast to the straight skeleton, the size of general plane bisector graphs need not be linear. A trivial upper bound is  $O(n^3)$ , as each node of the graph comes from a different triple of edges of  $P$ . The second anomaly is particularly undesirable for real-world roofs as rain water cannot run off.

Despite of the ambiguity of plane bisector graphs, their faces have a nice property which is easy to prove using the roof model.

**Lemma 3** *Each face  $f(e)$  of a plane bisector graph is monotone in direction of its defining edge  $e$ . That is, the intersection of  $f(e)$  with every line normal to  $e$  is connected.*

*Proof.* Let  $F$  be the roof facet corresponding to  $f(e)$ . Recall  $F \subset \Pi(e)$  and consider some line  $L$  in  $\Pi(e)$  normal to  $e$ . Obviously,  $L$  has slope 1, which is the maximum possible on the roof. Assume now that  $f(e)$  is not monotone in direction  $e$ . Then  $L$  can be chosen so as to leave  $F$  at some point  $x$  and to re-enter  $F$  at some higher point  $y$ . In between, the roof consists of facets contained in halfplanes different from  $\Pi(e)$ . Hence, when following the vertical projection of the segment  $xy$  on the roof, one traces segments of slope less than 1, thus ending up at a point vertically below  $y$ . This implies that the roof is not continuous – a contradiction.  $\square$

### 3 Islands

The concept of straight skeleton  $S(P)$  offers a unique way of constructing a roof avoiding the anomalies mentioned above, for a general layout  $P$  of ground walls. When viewing  $S(P)$  as

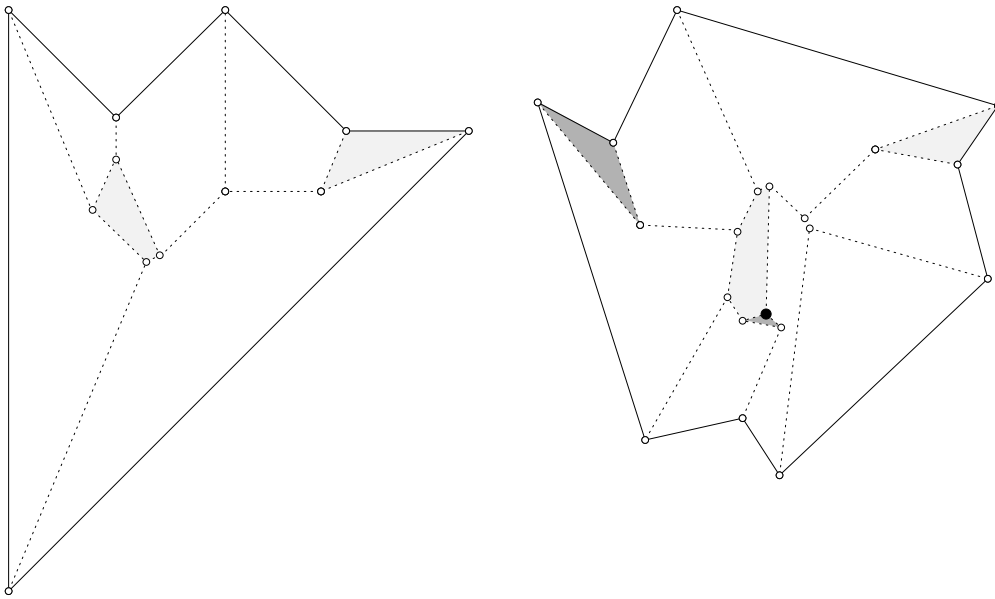


Figure 4: Disconnected faces and local minimum

a roof, the shrinking process defining  $S(P)$  has a nice physical interpretation. The roof is interpreted as an island with  $P$  delimiting the coast. Water level stands at plane  $\Pi_0$  and rises steadily during the shrinking process. Splits occur when the water surrounds local maxima of the island. The unique roof for  $P$  corresponding to  $S(P)$  will be called the *island* of  $P$ ,  $I(P)$ , in the sequel.

This flooding process – and the corresponding process of shrinking  $P$  – gives sense for non-island roofs, too. In fact, each roof for  $P$  defines a particular flooding process which uniquely defines a sequence of events. This will allow us to characterize  $I(P)$  among all possible roofs for  $P$ .

Let  $R$  be some roof for  $P$ . In the flooding process for  $R$ , we may encounter two new types of events beside edge events and split events. It is now possible that the water level reaches a local minimum of a facet at a corner  $c$  of  $R$ . If  $c$  is no local minimum of  $R$  then an edge parallel to some edge of  $P$  starts expanding there (inverse edge event). Else a triangular hole starts expanding from  $c$  (three simultaneous inverse edge events). Compare Figure 4.

**Lemma 4** *If  $R$  is a roof for  $P$  different from  $I(P)$  then  $R$  has a valley not incident to a (reflex) vertex of  $P$ . That is,  $R$  contains a valley that connects two corners of  $R$ .*

*Proof.* Note first that the flooding process starts in the same way for all possible roofs for  $P$ . That is,  $P$  starts to shrink in a unique manner. Now consider the first event that makes  $R$  differ from  $I(P)$ , and let  $c$  be the corresponding corner of  $R$ . Immediately before reaching  $c$ , water surrounds the part of  $R$  containing  $c$  and defines a polygon  $P'$  whose boundary delimitates the local coast. Obviously, the part of  $I(P)$  above  $P'$  is  $I(P')$ . As  $I(P')$  continues with the next-higher edge event or split event, and  $c$  is no corner of  $I(P')$ ,  $c$  corresponds to one of the two non-island types of event. Either such type involves an expansion of edges which can only take place at valleys. Hence either two or three valleys of  $R$  start at  $c$ , and the lemma is proved.  $\square$

**Theorem 2** *Let  $R$  be a roof for  $P$ . Then  $R = I(P)$  if and only if each valley of  $R$  is incident to  $P$ .*

*Proof.* Combine Lemma 2 and Lemma 4. □

It is easy to see that each roof for  $P$  has the same surface area. A natural question to ask is whether  $I(P)$  optimizes some other parameter among all possible roofs for  $P$ . However,  $I(P)$  achieves neither the maximum nor the minimum roof volume in general; see Figure 2 (shows  $I(P)$  in the middle) and Figure 5, respectively. These examples also reveal that neither the maximum nor the minimum global roof height is guaranteed. Still, the facets of  $I(P)$  obey a nice rule which is particular to  $I(P)$ .

Let  $R$  be any roof for  $P$ . For a point  $x$  on  $R$ , let  $g(x)$  denote the path that starts from  $x$  and follows the steepest gradient on  $R$ . We say that a facet  $F$  of  $R$  has the *gradient property* if, for every  $x \in F$ ,  $g(x)$  reaches the edge  $e$  defining  $F$  either in its interior or at a vertex.

**Theorem 3** *A roof  $R$  for  $P$  is the island of  $P$  if and only if each facet of  $R$  fulfills the gradient property.*

*Proof.* Assume  $R = I(P)$ . Let  $e$  be an edge of  $P$ , let  $F$  be its facet in  $R$ , and consider a point  $x \in F$ . By the monotonicity of faces stated in Lemma 3,  $g(x)$  reaches the boundary of  $F$  exactly once, at point  $y$ , say. If  $y \in e$  then we are done. Else  $y$  lies in a valley  $V$  of  $R$ . This is because valleys correspond to reflex arcs of the bisector graph, and only these arcs form an angle larger than 90 degree with  $e$ . It remains to be observed that  $g(x)$  follows  $V$  to its lowest point which, by Lemma 2, is a vertex of  $e$ .

Now assume  $R \neq I(P)$ . By Lemma 4,  $R$  contains a valley  $V$  whose lowest point is a corner  $c$  of  $R$ . Let  $F$  be a facet of  $R$  which has  $c$  as a local minimum, and let  $e$  be its defining edge. Then we can choose a point  $x \in F$  near  $V$  such that  $g(x)$  reaches and follows  $V$  and ends at  $c \notin e$ . □

A physical interpretation of Theorem 3 is that on  $I(P)$ , and only there, every raindrop that hits a facet  $F$  runs off to the edge defining  $F$ .

Theorem 2 and Theorem 3 can be used as definitions for  $I(P)$  and thus for  $S(P)$ . It would be elegant, however, to have a definition which does not resort to the explicit structure of  $I(P)$ . One approach that suggests itself is to try to express  $I(P)$  as the lower envelope of partial linear functions, each function being defined locally by an edge of  $P$  and its appropriate neighborhood. However, the example in Figure 5 shows us that such functions do not exist.

Consider the reflex vertex  $v$ , and let  $e$  be the edge incident to  $v$  whose facet in  $R(P)$  contains the point  $x$ . Let  $\phi(e) \subset \Pi(e)$  be the graph of some partial linear function for  $e$ . The facet of  $e$  in  $I(P)$  does not contain  $x$ , as  $I(P)$  is above  $\Pi(e)$  at  $x$ . So, if  $I(P)$  is the lower envelope of the functions  $\phi$ , then  $\phi(e)$  must not contain  $x$ . On the other hand, a change of  $P$  not in the neighborhood of  $e$ , namely moving the reflex vertex  $w$  slightly upwards, makes  $R(P)$  the valid island of  $P$ . Now  $\phi(e)$  has to contain  $x$  in order to ensure the envelope property for the modified polygon. This shows that  $\phi(e)$  cannot be defined without knowledge of  $I(P)$ .

This undesirable property of  $I(P)$  has far-reaching consequences. It reveals that  $S(P)$  is no Voronoi-diagram-like structure. To be more precise,  $S(P)$  cannot be interpreted as the Voronoi diagram of the edges of  $P$  for some locally defined distance function.

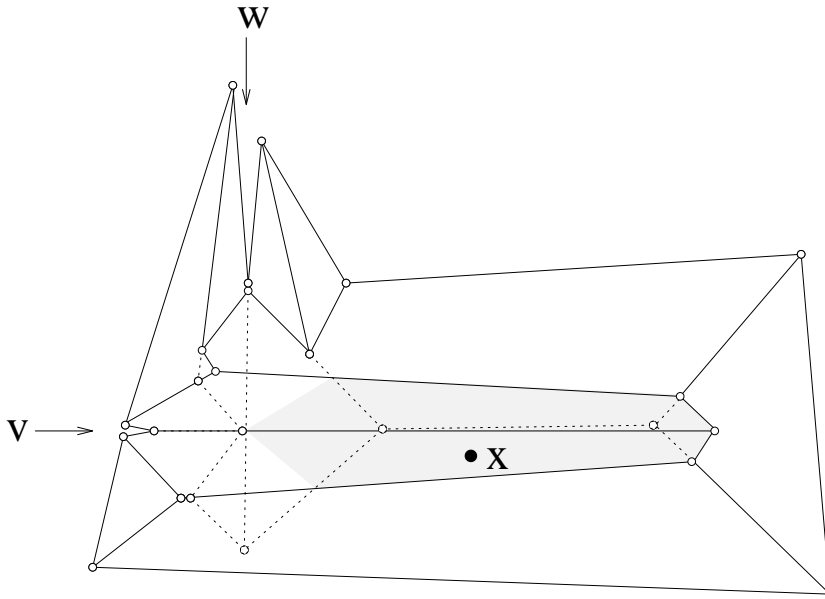


Figure 5:  $I(P)$  (dotted) dominates another roof  $R(P)$  (solid) at shaded area

## 4 Computing straight skeletons

We now turn to the problem of computing  $S(P)$  for a given  $n$ -gon  $P$ . Before diving into the description of the algorithm, let us rule out seemingly promising approaches.

We have argued that  $S(P)$  cannot be expressed as some Voronoi diagram of the edges of  $P$ . This excludes the well-developed machinery for constructing Voronoi diagrams from application. In particular, powerful techniques as divide-and-conquer or incremental insertion fail to work, as the straight skeleton is not defined for a subset of edges of  $P$ .

Still, the shrinking process for  $P$  or, more appropriately, the flooding process for  $I(P)$ , can be simulated by sweeping upwards a horizontal plane starting from  $\Pi_0$ . Edge events can be predicted easily, as the corresponding nodes of  $S(P)$  are the intersections of neighbored arcs. When holding events in a priority queue that reflects their height, a sequence of  $m$  consecutive edge events can be processed in  $O(n + m \log n)$  time. So  $O(n \log n)$  time suffices if  $P$  never splits, i.e., when  $I(P)$  has a single local maximum. This is particularly, but not exclusively, the case if  $P$  is convex.

Split events, however, cannot be detected locally. At each node that corresponds to a split event, a reflex arc  $a$  meets two convex arcs which both are not neighbored to  $a$  in the shrunk polygon immediately before. Note that knowing the edge  $e$  of  $P$  which is intersected by the prolongation of  $a$  does not help, as  $e$  might have moved out of  $a$ 's direction or even might have vanished before occurrence of the respective split event. Updating this information during the shrinking process seems costly in time and space: The edge aimed at by a reflex arc can change  $O(n)$  times, and there can be  $O(n)$  reflex arcs as  $P$  can have as many reflex vertices. Even initialization without using complicated ray shooting techniques in time below  $O(n^2)$  is unclear.

An obvious method for detecting the first split event for  $P$  is testing the shrunk polygon  $P(t)$  for self-intersection after each performed edge event  $t$ . If the test is affirmative, and only then, split events must have occurred between  $t$  and the edge event  $t'$  before. The very last event is an edge event, so all split events are found in this way. Fortunately, the split events



between  $t'$  and  $t$  can be read off the structure of  $P(t)$ .

Let us study what happens when  $P(t')$  shrinks to  $P(t)$ . At the first split event, a reflex vertex  $v$  sweeps across some boundary edge  $e$ . After the event, the polygon has been split into two polygons, called *lands*, which are connected by a triangle formed by  $v$  and the two newly created intersection points on  $e$ . The triangle is called a *bridge*, and the intersection points are called *articulation points*. If there are further split events before  $t$ , then this process repeats, splitting lands into smaller ones by introducing new bridges, until it ends up at  $P(t)$ . We make several observations on  $P(t)$ .

(1) Lands do not mutually overlap:  $P(t')$  would have self-intersections, otherwise.

(2) Bridges may overlap lands or other bridges.

(3) Bridges retain their initial triangular shape: Assume that a bridge  $B$  is created when a vertex  $v$  sweeps across an edge  $e$ , so that  $B$  is delineated by the edges  $vu$ ,  $vw$ , and  $e$ . If  $u$  or  $v$  sweep across  $e$ , or if a vertex of  $e$  sweeps across  $vu$  or  $vw$ , then this would cause an edge event that happens before  $t$ .

(4) Lands are connected by bridges in a tree-like fashion.

These observations suggest the following strategy. Traverse the tree of lands for  $P(t)$  and find all bridges, that is, find all articulation points. By (3), each split event between  $t'$  and  $t$  is manifested by a bridge. The time of occurrence of the event can be calculated from the shape of the bridge.

The major task, of course, is to detect all the articulation points for  $P(t)$ . By (4), there are only  $O(n)$  such points, whereas the total number of self-intersections of  $P(t)$  is  $O(n^2)$  by (2).

The algorithm detecting self-intersection of  $P(t)$  returns a pair of intersecting edges. One of them,  $e$ , belongs to a bridge by (1) and (2).  $e$  and an articulation point  $x$  on  $e$  can be found by intersecting both edges with the remaining edges of  $P(t)$ , and considering the interior-exterior information of the local intersection pattern.

It remains to be shown how an articulation point can be found that is neighbored to  $x$  in the tree of lands. To this end, we trace two chains  $C_1$  and  $C_2$  of edges of  $P(t)$ , starting at  $x$  and until either chain intersects itself or until  $C_1$  intersects  $C_2$ . Note that the latter is equivalent to a self-intersection of  $C_1 \cup C_2$ . The first self-intersection of a given chain is found by exponential search. That is, we test subchains  $C_i$  of length  $2^i$  until the answer is affirmative for some  $i$ . Binary search in the subchain  $C_i \setminus C_{i-1}$  then yields the desired answer. It is easy to see that, if  $m$  edges lie between  $x$  and the next articulation point  $y$  found, then  $O(m)$  edges are tested for intersection. Hence  $y$  is found in  $O(m \log m)$  time when one of the standard segment intersection algorithms [PS] is used, and all articulation points for  $P(t)$  are found in  $O(n \log n)$  time.

**Lemma 5** *Let  $t'$  be the edge event preceding the first split event for  $P$ , and let  $t$  be the first subsequent edge event. All the split events between  $t'$  and  $t$  can be determined (and also performed) in time  $O(n \log n)$ , provided  $t$  is already known.*

To speed up the determination of  $t$ , we may also use exponential search, namely on the sequence of consecutive edge events before  $t$ . If  $t$  is the  $k$ -th event then only  $O(\log k)$  tests for

polygon self-intersection are needed instead of  $O(k)$  tests. Each test takes time  $O(n)$  when the linear polygon triangulation algorithm in [C] is used.

**Lemma 6** *Let  $t$  be defined as in Lemma 5. If  $t$  is the  $k$ -th event for  $P$  then  $t$  can be found in time  $O(n \log k)$ .*

As already mentioned, all the edge events preceding  $t$  can be performed in  $O(k \log n)$  time. Recall also that, by Lemma 2, each split event uniquely corresponds to a reflex vertex of  $P$ . We finally obtain:

**Theorem 4** *Let  $P$  be an  $n$ -gon with  $r$  reflex vertices. The straight skeleton  $S(P)$  of  $P$  can be computed in time  $O(ns \log n)$  and space  $O(n)$ , where  $s \leq r$  counts the split events for  $P$ .*

Note that, by Lemma 5, running time will be better if there are many consecutive split events. If we are willing to spend an additional log-factor, then a much more practical algorithm is obtained. Its main part of implementation is a segment intersection detector.

## 5 Discussion

The contributions of this paper are two-fold: The introduction of a new internal structure for simple polygons, and the first systematic treatment of the problem of constructing a roof above a polygonal layout of ground walls.

The general advantages of the straight skeleton over the medial axis are its straight-line structure and its lower combinatorial complexity. Both structures reflect the shape of a polygon in a compact manner. However, the straight skeleton is more sensible to changes of the shape. Adding a reflex vertex with very small exterior angle may alter the skeleton structure completely. If this effect is undesirable then such vertices may be cut locally, without much changing the polygon and achieving exterior angles of at least 90 degrees.

A disadvantage of straight skeletons is the lack of a Voronoi diagram structure which makes tailor-made algorithms necessary. The  $O(ns \log n)$  time algorithm obtained here calls for improvement. The challenge is to find an algorithm with performance comparable to medial axis algorithms;  $O(n \log n)$  time, or even better if randomization may be used. A close-to-linear time algorithm is interesting also in view of the following fact. If  $S(P)$  is available then a triangulation of  $P$  (without Steiner points) can be constructed very easily in  $O(n)$  time. We first triangulate the (monotone) faces of  $S(P)$ , and then repeatedly remove nodes of constant degree and re-triangulate.

The straight skeleton provides a unique way of computing a roof given a general placement of ground walls. We have shown that roofs are highly ambiguous objects, and that constructing a roof is a non-trivial task. To our knowledge, the roof construction algorithm presented here is the first one in the literature. The algorithm has a simple implementation and should run quite efficiently in practice if the number of reflex points in the layout is not too large.

**Acknowledgements:** The second author would like to express thanks to G.L. Sicherman from AT&T Bell Labs. for drawing his attention to straight skeletons. Discussions on the presented topic with J.-D. Boissonnat, O. Devillers, M. Formann, R. Klein, D.T. Lee, G. Rote, and K. Varadarajan are gratefully acknowledged. Thanks also go to Th. Natschläger for implementing an algorithm for visualizing islands.

## References

- [C] B. Chazelle, *Triangulating a simple polygon in linear time*, Discrete&Computational Geometry 6 (1991), 485-524.
- [L] D.T. Lee, *Medial axis transformation of a planar shape*, IEEE Trans. Pattern Analysis and Machine Intelligence, PAMI-4 (1982), 363-369.
- [PS] F.P. Preparata and M.I. Shamos, *Computational Geometry: An Introduction*, Springer, New York, 1985.